EJN European Journal of Neuroscience

FENS Federation of European Neuroscience Societies

European Journal of Neuroscience, Vol. 42, pp. 2923–2933, 2015 doi:10.1111/ejn.13090

COGNITIVE NEUROSCIENCE

The selectivity of responses to red-green colour and achromatic contrast in the human visual cortex: an fMRI adaptation study

Kathy T. Mullen, Dorita H. F. Chang and Robert F. Hess

McGill Vision Research, Department of Ophthalmology, McGill University, 1650 Avenue Cedar, L11.513, Montreal, QC H3G 1A4, Canada

Keywords: hMT+, L/M cone opponent, V1, V4, VO

Edited by Guillaume Rousselet

Received 1 May 2015, revised 17 September 2015, accepted 23 September 2015

Abstract

There is controversy as to how responses to colour in the human brain are organized within the visual pathways. A key issue is whether there are modular pathways that respond selectively to colour or whether there are common neural substrates for both colour and achromatic (Ach) contrast. We used functional magnetic resonance imaging (fMRI) adaptation to investigate the responses of early and extrastriate visual areas to colour and Ach contrast. High-contrast red–green (RG) and Ach sinewave rings (0.5 cycles/degree, 2 Hz) were used as both adapting stimuli and test stimuli in a block design. We found robust adaptation to RG or Ach contrast in all visual areas. Cross-adaptation between RG and Ach contrast occurred in all areas indicating the presence of integrated, colour and Ach responses. Notably, we revealed contrasting trends for the two test stimuli. For the RG test, unselective processing (robust adaptation to both RG and Ach contrast) was most evident in the early visual areas (V1 and V2), but selective responses, revealed as greater adaptation between the same stimuli than cross-adaptation between different stimuli, emerged in the ventral cortex, in V4 and VO in particular. For the Ach test, unselective responses were again most evident in early visual areas but Ach selectivity emerged in the dorsal cortex (V3a and hMT+). Our findings support a strong presence of integrated mechanisms for colour and Ach contrast across the visual hierarchy, with a progression towards selective processing in extrastriate visual areas.

Introduction

In the visual cortex of the non-human primate brain, colour responses were initially thought to be confined in functionally segregated streams, in the blobs vs. the interblobs of V1 or the thin vs. the thick stripes and interstripes in V2 (Livingstone & Hubel, 1984, 1988; Levitt *et al.*, 1994). Subsequent evidence, however, tended to favour the merging and interaction of colour and achromatic (Ach) contrast into mixed, shape-processing pathways (Sincich & Horton, 2005; Economides *et al.*, 2011). In V1, colour-luminance neurons, tuned to orientation and spatial frequency, potentially provide a common form-processing pathway, with only a minority of lowpass, non-oriented (isotropic) neurons exclusively sensitive to colour (Thorell *et al.*, 1984; Lennie *et al.*, 1990; Leventhal *et al.*, 1995; Schluppeck & Engel, 2002; Friedman *et al.*, 2003; Johnson *et al.*, 2008; Shapley & Hawken, 2011; Li *et al.*, 2015). In V4, neurophysiological evidence suggests multiple functional organizations, including colour-selective neurons that process shape (Bushnell *et al.*, 2011; Bushnell & Pasupathy, 2012), segregated pathways with colour contrast or luminance contrast preferences, and colour-luminance shape-processing regions (Tanigawa *et al.*, 2010). In the human cortex, there is additional functional magnetic resonance imaging (fMRI) and psychophysical evidence for combined shape and colour processing (Sumner *et al.*, 2008; McDonald *et al.*, 2010; Seymour *et al.*, 2010; Gheiratmand & Mullen, 2014), although a retinotopic area in the ventral cortex anterior to V4 (labelled VO/V8) has been defined as highly responsive to colour contrast (McKeefry & Zeki, 1997; Hadjikhani *et al.*, 1998; Bartels & Zeki, 2000; Brewer *et al.*, 2005; Mullen *et al.*, 2007).

In this paper, we use an fMRI adaptation method to explore the selective vs. more integrated nature of the responses to red–green (RG) colour and Ach contrast in the human visual cortex, extending from V1 to the extrastriate areas (V2, V3v, V3d, V3a, hMT+ V4 and VO) of the dorsal and ventral streams. The fMRI adaptation technique is thought to act on the sub-populations of neurons represented within a single voxel and assumes that BOLD signals are reduced when two successive visual stimuli stimulate the same population but not when they activate different populations (Engel & Furmanski, 2001; Grill-Spector & Malach, 2001; Boynton & Finney, 2003; Engel, 2005; Fang *et al.*, 2005; Krekelberg *et al.*, 2006). As illustrated in Fig. 1a–c,

Correspondence: Kathy T. Mullen, as above.
E-mail: kathy.mullen@mcgill.ca

stimulus-selective adaptation is thought to identify specific neuronal populations within a voxel, potentially revealing the presence of selective neuronal responses. Voxels may contain predominantly colour-selective neurons (Fig. 1a), predominantly Ach-selective neurons (Fig. 1b), or a mixture of the two (Fig. 1c), and all will show selective adaptation in which the responses to the test stimuli are significantly more reduced by an adaptor of the same type than the opposite type. In contrast, voxels containing unselective neurons, such as colour-luminance cells that respond to both contrast types, will show unselective adaptation with responses reduced by both chromatic and Ach adaptation, as illustrated in Fig. 1d.

Materials and methods

Subjects

Thirteen healthy observers (10 female, three male) participated in this experiment, eight of whom were naive as to the purpose of the study. All observers had normal or corrected-to-normal vision. Informed written consent was gained from all participants prior to the commencement of the study. The study was conducted within the constraints of the ethical clearance from the Medical Research Ethics Committee of the University of Queensland for magnetic resonance imaging experiments on humans at the Centre for Magnetic Resonance and the McConnell Brain Imaging Centre at the Montreal Neurological Institute and Hospital, and conformed to the Code of Ethics of the World Medical Association (Declaration of Helsinki). All participants were screened for fMRI contraindications.

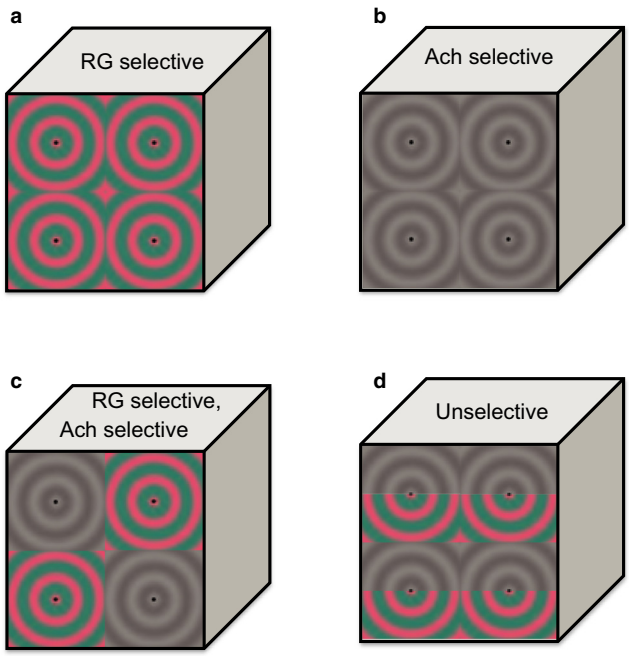

FIG. 1. Schematic illustrating the principle of how selective and unselective adaptation can identify specific neuronal populations within a voxel. (a) Voxels containing neurons selective for RG chromatic contrast are expected to show selective RG chromatic adaptation. (b) Voxels containing neurons selective for Ach contrast are expected to show selective Ach adaptation. (c) Voxels can show both types of selectivity compatible with the presence of both types of neurons. (d) Voxels containing unselective neurons responsive to both colour and Ach contrast are expected to show unselective adaptation, in which same-adaptation and cross-adaptation are similarly effective. In reality, various combinations of (a–d) may occur. The radial pattern icons are reduced versions of the stimuli used.

Stimuli and colour space

The stimuli were radial sinewave gratings (0.5 cycles/degree), with contrast sinusoidally phase reversing at 2 Hz (Mullen *et al.*, 2007, 2008). All stimuli were presented in a temporal Gaussian contrast envelope (sigma 125 ms). RG chromatic and Ach stimuli were used that isolated the L/M cone opponent and luminance (Ach) post-receptoral mechanisms, respectively. The cone contrasts of the stimuli were set to 4.0% for the RG condition and 22% for the Ach condition, creating highly visible stimuli and maximizing signal strength. The stimulus size was 19° (full width) by approximately 19° (full height). A small fixation dot was present in the centre of the stimulus. A smaller version of these stimuli with fewer cycles is shown in Fig. 1a–c. The radial stimulus arrangement permitted a spatially narrow band stimulus to be displayed at a relatively low spatial frequency. A spatial frequency of 0.5 cycles/degree at 2 Hz was chosen to avoid luminance artefacts generated by chromatic aberration in the chromatic stimuli (Bradley *et al.*, 1992; Cottaris, 2003) and because this is an optimal spatial and temporal frequency for capturing both colour and Ach responses with these conditions disadvantaging neither colour nor Ach contrast sensitivity (Mullen, 1985).

The stimulus chromaticity was defined using a three-dimensional cone contrast space in which each axis represented the quantal catch of the L, M and S cone types normalized with respect to the white background (i.e. cone contrast). The chromaticity was given by the vector direction and contrast by vector length within this space. The isoluminance of the RG stimuli was determined for each subject individually based on perceptual minimum motion settings as previously described (Mullen *et al.*, 2007, 2010).

Apparatus and calibrations

The stimuli were generated using Matlab with extensions from PsychToolbox (Brainard, 1997; Pelli, 1997) on a Macintosh computer and back-projected on a screen using an LCD projector (NEC VT580, resolution 1024 × 768, frame rate 60 Hz, mean luminance 270 cd/m^2) placed at the back of the bore 1 m from the participant. For the psychophysical experiments used to determine detection threshold and isoluminance, stimuli were generated using a VSG 2/5 graphics board with 15 bits of contrast resolution (Cambridge Research Systems Ltd, Rochester, UK) housed in a Pentium PC computer and displayed on a CRT monitor (Diamond Pro 2030). Both projection and CRT displays were linearized and colour calibrated as previously described (Mullen *et al.*, 2007; Michna & Mullen, 2008). The cone contrast gamut was most limited in the RG direction, with an upper cone contrast limit for the projection system of around 5% for the RG stimuli, depending on the calibration data, projector settings, and isoluminant point.

Experimental protocols

Test stimuli and control for attention

The test stimuli were presented time-locked to the acquisition of fMRI volumes (TR of 3 s) and were designed to control for attention, as previously described (Mullen *et al.*, 2007, 2010). Briefly, in each 3 s test trial, observers performed a two-interval, two-alternative forced-choice contrast-discrimination task. Stimuli were presented twice with a near-threshold contrast difference between them (all other aspects being the same) and the subject indicated with a button press the interval with the higher stimulus contrast. The contrast difference between the two stimuli was fixed at 30% (± 15%

of mean) for all participants, yielding an overall average discrimination of ~84% correct. Each stimulus was presented within a 500 ms time window in a temporal Gaussian contrast envelope (sigma of 125 ms) with an interstimulus interval of 500 ms. The subject's response was given in the remaining 1.5 s. Fixation blocks consisted of a small sinusoidal ring of the same chromaticity as the stimulus (modulated at 2 Hz) surrounding a small fixation spot. During these blocks, participants performed an identical contrast discrimination task with the fixation stimulus.

Scan protocol

The chromatic or Ach adaptation scans were conducted in separate sessions on separate days. As illustrated in the schematic of Fig. 2, each run was composed of three sequential repeating blocks: (1) adaptation/no-adaptation block (12 s) with continuous presentation of the adapting stimulus or a blank, no-adapt field; (2) test block (18 s) consisting of six sequential test stimulus presentations of: (i) all RG stimuli, (ii) all Ach stimuli, or (iii) alternating RG and Ach stimuli; and (3) fixation block (9 s). Blocks 1–3 were repeated three times with the same adaptor condition (adapt or no-adapt) but with the three different test blocks (i–iii) in pseudo-random order. Next, the adaptor type was changed, from adapting stimulus to no-adapt or vice versa, and the series repeated. The whole adapt plus no-adapt sequence was repeated three times, starting pseudo-randomly with the adaptation or no-adaptation block. Hence, in one scan of approximately 12 min, the adaptor and the blank were each presented nine times. Subjects completed a minimum of four repeated scans per adaptor (RG or Ach) and each subject performed the same number of scans per condition. Subject data from all runs were averaged before being entered into group-wise analyses. We defined the adaptation as long term as it involved more than 10 s of exposure to an adaptor (Krekelberg *et al.*, 2006). The mixed test condition

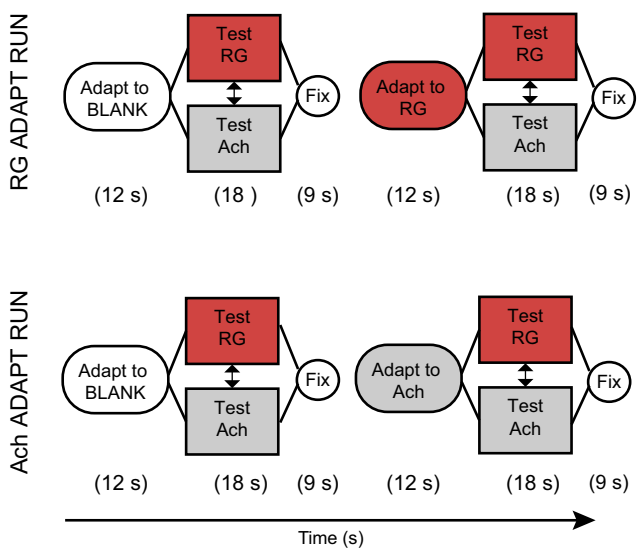

FIG. 2. Schematic time-line of the scanning protocol. One scan consisted of the following sequence: adaptation block (12 s) with continuous presentations of either the adapting stimulus or a blank grey field (no-adapt), test block (18 s) in which one of three types of test blocks was presented (all RG stimuli, all Ach stimuli, or a mixed presentation of alternating RG and Ach stimuli), and fixation block (9 s). This sequence was repeated for each of the three test stimuli in pseudo-random order before switching to the other adapting condition (no-adapt vs. adapt). The paired adapt, no-adapt sequences were repeated three times. The scan started with a pseudo-randomized adapt or no-adapt condition (TR = 3 s).

(iii) using alternating test stimuli was inserted as part of a different experiment to test for shorter term adaptation effects produced by the repeated brief (1 s) exposures to the test stimulus pairs during the 18 s test block. As we found no difference between the BOLD responses to the mixed and all-RG or all-Ach stimuli across the time course of the stimulus block in any visual area, we concluded that short-term, self-adaptation from the multiple test stimuli presentations was insignificant and we did not pursue this further.

Magnetic resonance imaging

Initial fMRI data on four of the 13 subjects were acquired using a 4T Bruker MedSpec system at the Centre for Magnetic Resonance (Brisbane, Australia) as previously described (Mullen *et al.*, 2007, 2008), and subsequently using the same acquisition parameters on a 3T Siemens TIM Trio at the McConnell Brain Imaging Centre of the Montreal Neurological Institute. A 32-channel SENSE head coil (3T) was used for radiofrequency transmission and reception (Vaughan *et al.*, 2002). EPI data (gradient echo-pulse sequences) were acquired from 44 slices (whole brain coverage; TR, 3000 ms; TE, 30 ms; 3.0 mm^3 resolution). Slices were oriented parallel to the calcarine sulcus. Head movement was limited by foam padding within the head coil. For each participant, a high-resolution three-dimensional T1 image was acquired using an MP-RAGE sequence (TI, 1500 ms; TR, 2500 ms; TE, 3.83 ms; spatial resolution, 0.9 mm^3). Localizations of the regions of interest (ROIs) were performed in separate sessions with identical acquisition parameters.

Pre-processing of magnetic resonance images

The magnetic resonance imaging data were processed using Brain Voyager QX 2.6.1 (Brain Innovations, Maastricht, The Netherlands). The anatomical data of each observer were used for cortex reconstruction, inflation, and flattening. The initial volume of each functional run was discarded in order to eliminate the effects of start-up transients in the data. Functional data were pre-processed using slice-time correction, three-dimensional motion correction (six parameters, trilinear/sync interpolation), spatial smoothing (Gaussian filter, full-width at half maximum, 5 mm), linear trend removal, and highpass filtering (three cycles per run cut-off). The functional images were then aligned to each participant's anatomical data and transformed into Talairach space (Talairach & Tournoux, 1988). For each observer, functional data between different sessions were co-aligned. All volumes of each observer were aligned to the first functional volume of the first run of the session. This ensured accurate registration across sessions.

Identification of regions of interest

The visual cortical regions V1, V2, V3v, V3d, V3a and V4 were identified for each participant using rotating wedge stimuli and expanding and contracting concentric rings (Engel *et al.*, 1994; Sereno *et al.*, 1995) as described in previous work (Mullen *et al.*, 2007, 2010), and in accordance with known anatomical landmarks. The putative human motion complex hMT+ was identified as the set of voxels in the occipital cortex that responded significantly more to a high-contrast flickering (16 Hz) checkerboard stimulus than to a stationary checkerboard (Dumoulin *et al.*, 2000). (See Table S1 for all MT coordinates). Area VO was identified by contrasting, in a block design, responses to isoluminant RG (L/M) and blue–yellow (S) counter-phasing rings with responses to Ach rings. Localizer stimuli had the same parameters as the experimental stimuli (0.5 cy-

cles/degree, 2 Hz, stimulus diameter of 19°), and were matched in cone contrast (4%). This revealed the relative contrast responsivity of voxels to isoluminant colour vs. Ach contrast. Due to the proximity of this region to retinotopic V4, any overlapping voxels were excluded. Using this localizer, we were able to identify a VO cluster in nine of 13 subjects. (Table S1 gives coordinates for VO and V4). For the remaining four subjects, who were no longer available or for whom we could not reliably identify this region, VO was defined as a spherical (6 mm) ROI centred on mean Talairach coordinates identified previously by our group (Mullen *et al.*, 2007) and adjusted for each subject so that there was no overlap between VO and the retinotopically defined areas (e.g. V4). The definition of VO from Mullen *et al.* (2007) is functional and includes all voxels with greater colour than Ach sensitivity (t-value > 3) adjusted for each subject to exclude overlap between VO and the retinotopically defined areas. Thus, for all participants, VO was defined as a colour-sensitive region that lies beyond hV4 but may contain parts of several ventral occipital visual areas (Brewer *et al.*, 2005). In addition, we compared results using two definitions of VO in five subjects, i.e. a spherical ROI as used here and one functionally defined based on a greater response to colour than Ach stimuli at equivalent cone contrasts. We found no difference in the averaged chromatic responses or the adaptation effects between the two.

Functional magnetic resonance imaging and statistical analyses

Whole-brain activity maps

Whole-brain, group-level responses were analysed using GLM random-effects analyses. All GLM analyses included regressors for each experimental condition, defined as square-wave regressors for each stimulus presentation block convolved with a gamma function to approximate the idealized haemodynamic response (taking into account a 3 s haemodynamic lag). The time course signal of each voxel was then modelled as a linear combination of the different regressors (least-squares fits) and the regressor coefficients were used for contrasts of the different experimental conditions. Contrasts were performed independently for RG chromatic and Ach adaptation runs, differencing responses to the test stimuli following adaptation vs. no adaptation. A particular contrast revealed voxels with suppressed neural signals for a test stimulus following the adaptation period vs. the blank, no-adapt period.

Region of interest analyses

For each ROI, we computed the percent BOLD signal (percent signal change) by extracting time courses from each voxel and normalizing to the baseline given by the mean signal intensity during the fixation blocks. Hence, all signals within a particular scan were defined as a percent signal change relative to the mean fixation signal. We determined the mean response for a particular condition by computing the mean response across a set of voxels within the ROI (maximum $n = 300$) selected on the basis of a significant ($P < 0.05$) response to stimulus presentations relative to fixation for the test stimuli (i.e. RG, Ach) preceded by no-adaptation intervals. For each run (RG-adapt or Ach-adapt), the mean percent signal change was computed separately for each test (RG, Ach, Mix) independently for adaptation and no-adaptation intervals. For each ROI, the effect of adaptation on the response to each test stimulus (signal loss) was calculated as the difference in response between the no-adapt and adapt conditions (no-adapt – adapt) and was calculated independently for each adaptor type (RG, Ach). Selective adaptation was indicated by a greater signal loss arising from an adaptor that was the same as the test compared with one that was different from the test (same adaptation – cross-adaptation). The effects of adaptation on each test stimulus were analysed using a full repeated-measures ANOVA comparing the effects of adaptation (no-adapt/adapt) and the adaptor type (RG/Ach) across all eight ROIs, independently for each of the RG and Ach tests. *Post-hoc* comparisons for main effects and significant interactions were performed with follow-up two-way ANOVAS and Bonferroni-corrected t-tests.

Results

During each scan, subjects viewed RG or Ach test stimuli following either a period of no-adaptation, in which a grey uniform field was presented, or a period of adaptation, in which an adapting stimulus was presented (Ach or RG, depending on the scan).

Group-level activity maps

In Fig. 3 we show group-level results from the whole-brain, GLM analyses to illustrate the signal loss produced by the adapting stimuli. We show the average statistical maps for all 13 subjects superimposed on flattened cortical surfaces of both hemispheres for one participant (DC), with the regions (V1, V2, V3d, V3A, V3v, V4, the putative human motion complex, hMT+, and VO) delineated for this subject and presented for illustrative purposes. Note that computations for individual subjects were performed using their own, independently identified ROIs. In this figure, t-values represent the differences between the responses following the adapt and no-adapt conditions (no-adapt – adapt) for each test stimulus, with the red–yellow scale indicating a significantly smaller response after adaptation compared with no-adaptation. Results obtained using the chromatic adaptor are shown in the top panels (Fig. 3a and b), and using the Ach adaptor in the lower panels (Fig. 3c and d), with results for the chromatic test stimuli in the left panels (Fig. 3a and c), and for Ach test stimuli in the right panels (Fig. 3b and d). The results show that adaptation caused significant signal loss in all conditions. Overall, this loss tended to be more extensive and to occur over a larger cortical area when the adapting and the test stimuli were the same, as in Fig. 3a (colour adaptor, colour test) or Fig. 3d (Ach adaptor Ach test), compared with when they were different (cross-adaptation in Fig. 3b and c). Thus, there is evidence for both selective (same) adaptation and unselective (cross-) adaptation depending on the conditions and brain areas involved. In order to better quantify the adaptation effects across cortical areas and between conditions, we next computed the percent signal changes within each ROI.

Region of interest-based percent signal change

Figure 4 shows (group-averaged) raw time series for an example area (V1) during the adaptation blocks (first four TRs, 1–4) and test blocks (next six TRs, 5–10). Results are shown for scans with RG chromatic (Fig. 4a and b) and Ach (Fig. 4c and d) adaptation. During the adaptation period, responses for both the RG and Ach adaptor were very similar (see also Fig. S4 for other ROIs). During the test period, for stimuli presented in the no-adapt conditions, responses initially rose (TR 5–7) and then slightly declined (TR 8–10). For test stimuli presented after adaptation, a very different trend occurred with signals starting high and gradually weakening (TR 5–10). The effect of adaptation is revealed by the separation between

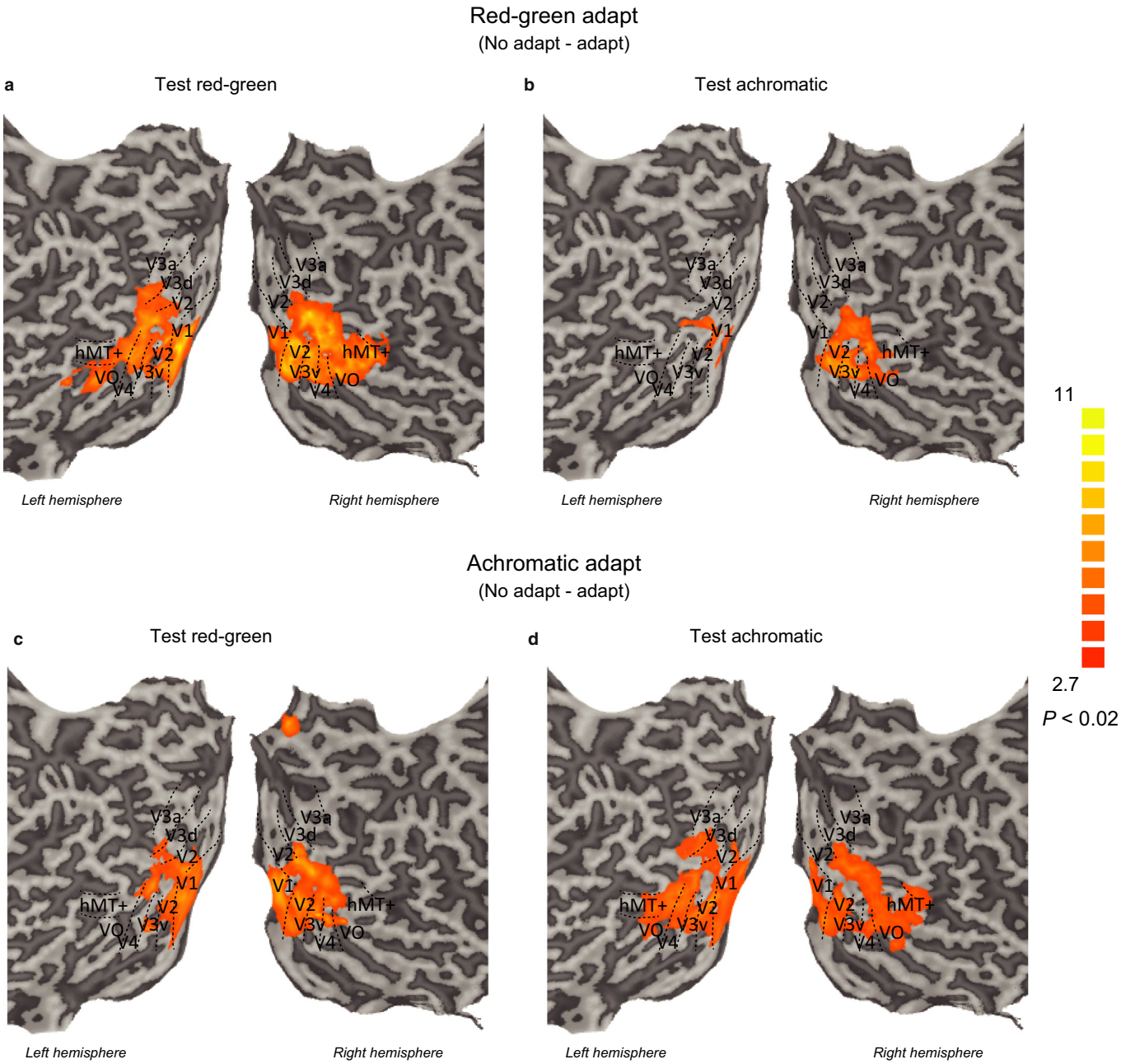

FIG. 3. Group contrasts between the adaptation and no-adaptation conditions. Results of the GLM analyses (random effects), contrasting responses after adaptation with no-adaptation (no-adapt – adapt), superimposed onto representative flat maps of left and right hemispheres. Results are shown for RG-colour adaptors (a and b) and Ach adaptors (c and d), for RG and Ach test stimuli as marked. The analyses show that adaptation is greater when the adaptor and test are the same (a and d, same adaptation) compared with when they are different (b and c, cross-adaptation). The flat maps show the location of the retinotopic areas, the human motion complex (hMT+), and VO, indicated by the dashed lines, obtained from one representative participant (DC). Regions were defined for each participant using independent localizers. Sulci are coded in darker grey than the gyri.

the adapt (solid) and no-adapt (dashed) curves. For example, the separation of the dashed and solid red lines shows the effect of chromatic (Fig. 4a) or Ach (Fig. 4c) adaptation on the response to colour contrast, demonstrating a clear signal loss in the responses to the stimuli after adaptation. Additionally, for this particular ROI, there was similar signal loss following chromatic or Ach adaptation for both test stimuli, suggesting unselective adaptation. For this and all other ROIs, test responses and adaptation effects were computed by averaging across the last five TRs of the test period (TR 6–10), excluding the first test TR (TR 5).

Responses to red–green colour and achromatic contrast without adaptation

In the example region presented in Fig. 4 (V1), the chromatic response (dashed red line) tended to be greater than the Ach (dashed black line) response. However, an examination of the mean responses to the test stimuli following no (blank) adaptation revealed that this effect varied with visual area. In Fig. 5, we present the raw data for the Ach and RG tests following no-adapt (white bars) and after RG-adapt (Fig. 5a, coloured and grey bars) or

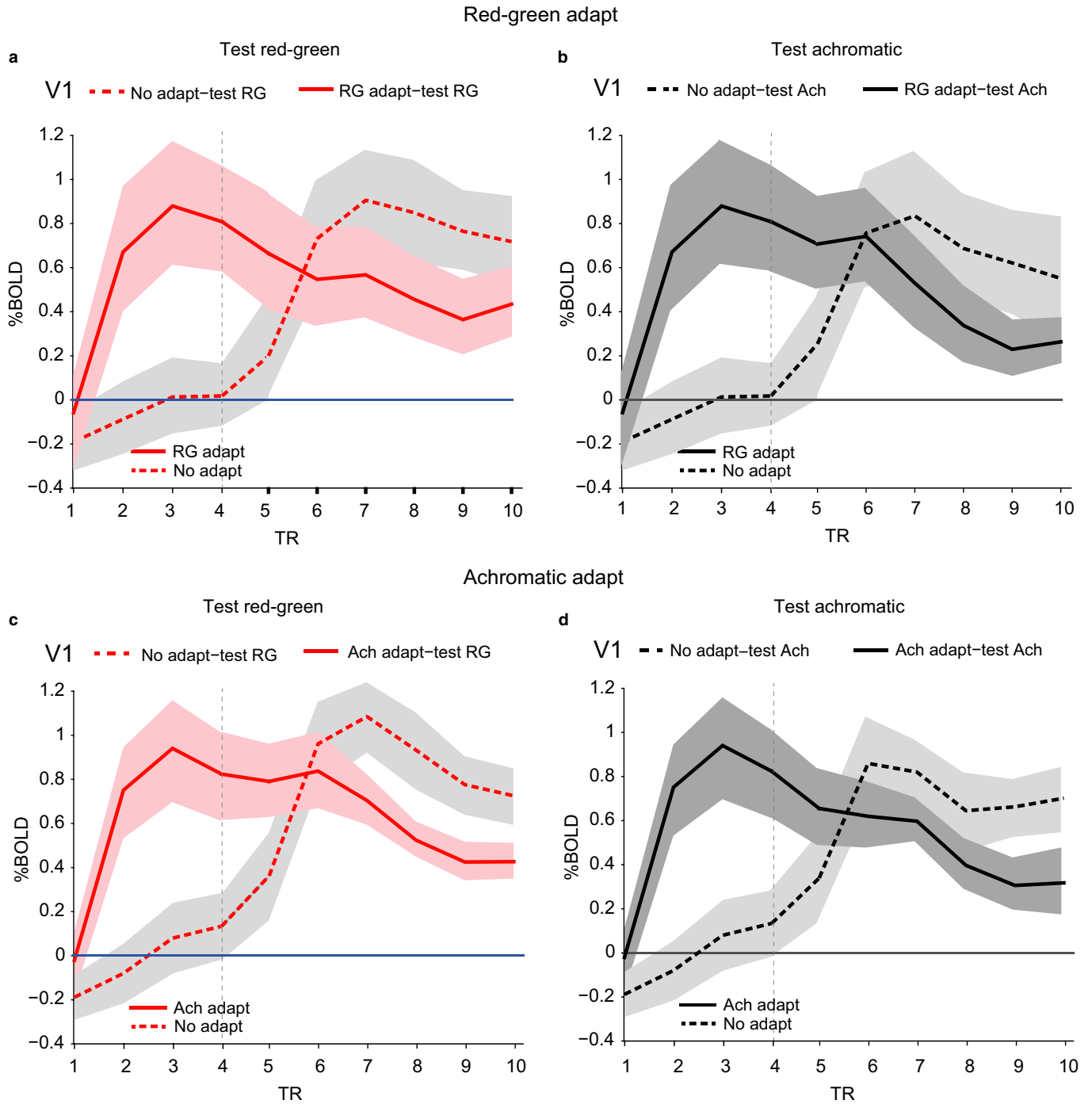

FIG. 4. Time series data for area V1. % BOLD plotted as a function of time (in TRs) for Ach (black lines) and RG (red lines) test stimuli, with no adaptation (dashed lines) or after adaptation (solid lines) for RG adaptation (a and b) and Ach adaptation (c and d) scans. Adapting stimuli were presented in TRs 1– 4 and test stimuli in TRs 5–10, demarcated by the vertical dashed line. Responses (% BOLD) are normalized to the average of the fixation presentations. Note that, in computations of the ROI-based percent signal changes, we consider only the mean response between TR 6 and TR 10 (see Materials and methods), excluding the first test TR after the adaptation period (TR 5). Data represent the mean response across subjects and shaded areas show the 95% confidence intervals.

Ach-adapt (Fig. 5b, coloured and grey bars). As revealed in these figures, there is a tendency for stronger responses to colour than to Ach contrast in V1/V2 and in some areas of the ventral pathways, but relatively weaker colour responses in the areas of the dorsal pathways, preferences that have been well established in previous studies when the cone contrasts of stimuli are matched (Mullen *et al.*, 2007). A statistical analysis of our no-adapt data [repeated-measures ANOVA on percent signal change for ROI × Adaptor runs (RG/Ach) × Test (RG/Ach)] indicated a significant main effect of test ($F_{1,12} = 9.3$, $P = 0.01$), a significant main effect of ROI ($F_{7,84} = 20.3$, $P < 0.001$), and a significant test by ROI interaction ($F_{7,84} = 13.6$, $P < 0.001$). *Post-hoc* Bonferroni-corrected comparisons indicated that the interaction was due to the fact that the chromatic response

was greater than the Ach response in areas V1, V2, V3v, V4, and VO ($P < 0.005$ for all). The no-adapt conditions were the reference by which we measured the effect of adaptation. They were also important for establishing that the different visual areas had a response to the stimuli used and all areas showed a significant response.

Effect of adaptation

The adaptor causes a reduced response to the test stimuli in most visual areas (Fig. 5, coloured and grey bars). In order to reveal these results better we calculated the signal loss due to adaptation by differencing the test responses following adaptation and no adaptation (no-adapt minus adapt). These differences are plotted in Fig. 6 for each test stimulus. We were interested in whether adaptation of the RG and Ach tests occurred across the visual cortical network, or at least across our ROIs.

We first entered our data in terms of raw percent signal change into a full repeated-measures ANOVA [(2) Adaptation (Blank/Adapt) × (2) Adaptor (RG/Ach) × (8) ROI] for each of the RG and Ach tests. The analyses for both the RG and Ach tests indicated a significant main effect of Adaptation (RG test: $F_{1,12} = 40.9$,

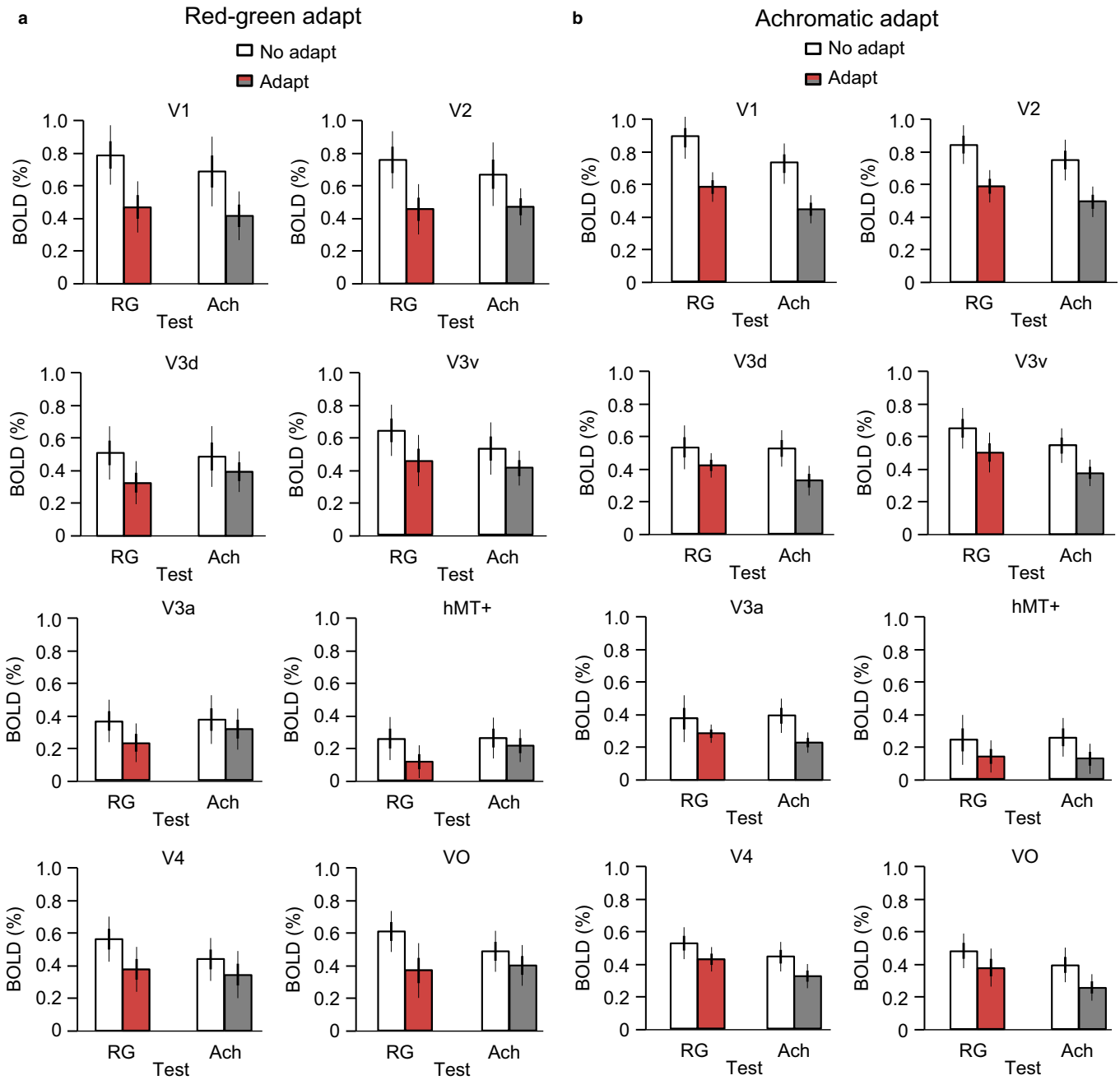

FIG. 5. ROI-based analysis for RG adaptation and no-adaptation conditions. (a) % BOLD is plotted for the two test stimuli in the RG adaptation condition: RG test after adaptation (coloured bars) and Ach test after adaptation (grey bars), and white bars show the corresponding no-adapt response to each test. Each panel represents a different visual area as marked. (b) % BOLD is plotted for the two test stimuli in the Ach adaptation condition, with symbols as described above. All results are the subject average with thick error bars showing ± 1 SE and thin extensions showing the 95% confidence intervals. Data are given in Tables S2-S9.

$P < 0.001$; Ach test: $F_{1,12} = 37.4$, $P < 0.001$), indicating that overall responses were lower following adaptation vs. no adaptation, a significant Adaptor by ROI interaction (RG test: $F_{7,84} = 2.5$, $P = 0.021$; Ach test: $F_{7,84} = 2.6$, $P = 0.019$) and a significant Adaptation by ROI interaction (RG test: $F_{7,84} = 11.8$, $P < 0.001$; Ach test: $F_{7,84} = 8.7$, $P < 0.001$). For both tests, the Adaptor by ROI interaction was not pursued further, as we were not interested in comparing variations in responses collapsed across no-adapt/adapt conditions. For the adaptation by ROI interactions, the differences in magnitude of the adaptation effect across ROIs may simply have reflected the differences in overall responsiveness of the areas to chromatic or Ach contrast (i.e. an ROI with higher responses without adaptation may show greater signal loss when no-adapt and adapt responses are differenced). Hence, we also represented the data in terms of a proportional loss normalized to the raw (no-adapt) signal (Fig. S1), which showed a similar pattern of results but with much less variation across ROIs.

Our main interest was to compare, within each ROI, the effects of the two adaptors on each test to determine how selective the adaptation was. For this, we entered our data into an ANOVA [(2) Adaptation (Blank/Adapt) × 2 (Adaptor (RG/Ach))] for each ROI and for each test. These analyses were adjusted to control for multiple comparisons for the RG-adapt and Ach-adapt.

Red–green test

Considering the results for the RG test first, the ANOVAs for the early visual areas V1 to V3 indicated significant main effects of Adaptation (V1: $F_{1,12} = 85$, $P < 0.001$; V2: $F_{1,11} = 62.4$, $P < 0.001$; V3d: $F_{1,12} = 16.0$, $P = 0.002$; V3v: $F_{1,12} = 41.4$, $P < 0.001$), no significant main effect of Adaptor, nor interaction, indicating unselective adaptation with both RG and Ach adaptors causing similar signal loss for the RG test, as can be seen in Fig. 6a. Similarly, the analysis for the two dorsal areas, V3a and hMT+, revealed significant main effects of Adaptation (V3a: $F_{1,12} = 8.0$, $P = 0.015$; hMT+: $F_{1,12} = 13.5$, $P = 0.003$), but no significant main effect of Adaptor, nor interaction, again suggesting unselective adaptation of the colour test. Interestingly, however, the ANOVAs for the two ventral regions, V4 and VO, showed a different pattern. For these regions, the analysis indicated a significant main effect of Adaptation (V4: $F_{1,12} = 29.5$, $P < 0.001$; VO: $F_{1,12} = 21.6$, $P < 0.001$), and a significant Adaptation by Adaptor interaction (V4 marginally significant: $F_{1,12} = 5.1$, $P = 0.04$; VO: $F_{1,12} = 7.4$, $P = 0.018$). The interaction reflected the fact that the signal loss for the colour test in these ventral regions, in particular VO, was greater following RG adaptation than Ach adaptation. This showed colour selectivity in the ventral areas, particularly VO, as can be seen in Fig. 6a.

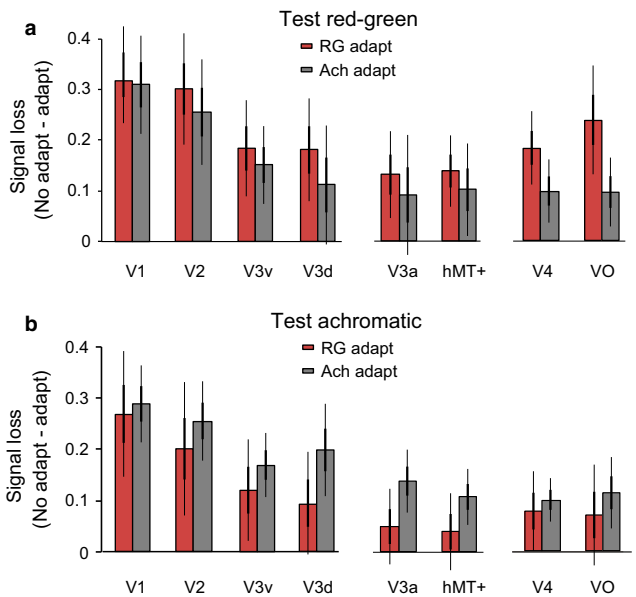

FIG. 6. Signal loss following adaptation plotted by test stimulus. Signal loss is the difference in % BOLD for the no-adapt minus the adaptation runs for (a) the RG test stimuli with an RG adaptor (same-adaptation, coloured bars) or Ach adaptor (cross-adaptation, grey bars), and (b) the Ach test stimuli with an RG adaptor (cross-adaptation, coloured bars) or Ach adaptor (same-adaptation, grey bars). Selectivity of the response for RG test stimuli (a) or Ach test stimuli (b) is indicated by the difference in signal loss between the same-adapt and cross-adapt conditions for each test stimulus. Results are the subject average with thick error bars showing ± 1 SE and the thin extensions showing the 95% confidence intervals. Statistical treatments are described in the text.

Achromatic test

We next consider the analyses for the Ach test presentations (Fig. 6b). The ANOVA for the early visual areas V1 to V3 indicated significant main effects of Adaptation (V1: $F_{1,12} = 66.1$, $P < 0.001$; V2: $F_{1,11} = 41.5$, $P < 0.001$; V3d: $F_{1,12} = 28.6$, $P < 0.001$; V3v: $F_{1,12} = 38.9$, $P < 0.001$), but no significant main effect of Adaptor, nor interaction, indicating unselective adaptation, as was also found for the RG test. In the dorsal areas V3a and hMT+, the analysis indicated significant main effects of Adaptation (V3a: $F_{1,12} = 17.6$, $P = 0.001$; hMT+: $F_{1,12} = 8.3$, $P = 0.01$). Although the two-way interaction approached, but not did not reach, statistical significance (V3a: $F_{1,12} = 3.9$, $P = 0.07$; hMT+: $F_{1,12} = 4.2$, $P = 0.06$), an examination of Fig. 6b indicates that this reflects a trend for Ach selectivity in these two dorsal regions. We also note that, in these two regions, the Ach signal loss is small for chromatic adaptation with the confidence intervals passing through zero, indicating a very weak adaptation effect. Finally, the ANOVAs for the ventral regions V4 and VO indicated a significant main effect of Adaptation (V4: $F_{1,12} = 16.9$, $P = 0.001$; VO: $F_{1,12} = 9.03$, $P = 0.011$), but no interaction, suggesting that, unlike the results for the RG test, there was unselective adaptation to the Ach test in the ventral cortex.

To compare and visualize the selectivity of the adaptation effects at the individual subject level, we generated scatterplots for each ROI, plotting for each participant the signal loss following the Ach adaptor vs. the signal loss following the RG adaptor (Fig. S2). For the RG test stimulus, in the early visual areas data points were almost evenly scattered and showed no particular trend for selective adaptation. In ventral regions, in particular VO, many subjects showed RG-selective adaptation, which was congruent with the group-level trend (c.f. Fig. 6a). For the Ach test stimulus, individual subject losses again appeared unselective in early visual areas. By the dorsal cortex, however, the majority of subjects showed Ach-selective adaptation, congruent with the group-level trend (c.f. Fig. 6b).

Supplementary analyses

We consider two possible factors that may have an influence on the above patterns of results. First, as our test period (18 s) was relatively long we asked whether adaptation effects may diminish in the latter half of the test period relative to the first half. We recomputed the signal loss for the test stimuli considering the first 6 s of the test window ('early test'), or the final 9 s of the test period ('late test'). The results (Fig. S3a and b) showed that the pattern of adaptation

was similar for both portions of the test period; in fact, signal losses and selectivity appeared to be somewhat greater in the second half. Hence, the adaptation effect was relatively long lasting.

Second, we considered whether any persistence of the adaptor response into the test period could affect our pattern of results, and in particular the selectivity of adaptation. As we were comparing the test response between two adaptors, it is possible that our adaptation effects may have been artificially inflated or suppressed if one adaptor produced a greater response than the other. To address this issue we calculated the raw signal of the RG and Ach adaptors during the adapting window (Fig. S4). Analysis of these data using a 2 (adaptor) × 8 (ROI) repeated-measures ANOVA confirmed that the two adaptor responses did not differ significantly ($F_{1,12} = 0.82$, $P = 0.38$).

Discussion

We have investigated the adaptation and selectivity of RG chromatic and Ach responses across the human visual cortex. Both chromatic and Ach test responses are adapted by both RG and Ach adaptor types, suggesting the presence of unselective mechanisms across many areas that span the visual hierarchy. However, we note two contrasting effects in our data for the RG and Ach test responses. For both, selectivity develops within the extrastriate visual areas but with a functional dissociation along the dorsal and ventral pathways. In particular for the RG chromatic response, we observe a trend towards greater RG selectivity in the two ventral extrastriate areas, V4 and most noticeably in VO. For the Ach test response, we instead observe selective responses developing in several areas of the dorsal cortex and in particular V3A and hMT+. These results suggest that there is not a simple cascade of adaptation effects flowing through the visual system. As dorsal vs. ventral areas, and higher vs. lower areas, have different patterns of adaptation, adaptation is unlikely to be simply inherited by one area from another.

The fMRI adaptation technique acts on sub-populations of neurons represented within a single voxel and assumes that BOLD signals are reduced when two successive stimuli stimulate the same population but not when they activate different populations (Kourtzi & Kanwisher, 2000; Engel & Furmanski, 2001; Grill-Spector & Malach, 2001; Boynton & Finney, 2003; Kourtzi *et al.*, 2003; Engel, 2005; Fang *et al.*, 2005; Krekelberg *et al.*, 2006). Thus, stimulus-selective adaptation potentially reflects the presence of selective neuronal responses within a voxel. It assumes that the adaptation effect originates within the driver neurons (see, for a review, Krekelberg *et al.*, 2006). There is good evidence that long-term adaptation in fMRI is within-channel specific as it has orientation-tuned characteristics in V1 (Engel, 2005; Fang *et al.*, 2005) and direction-tuned characteristics in area hMT+ (Huettel *et al.*, 2004) compatible with the known characteristics of the driver neurons in these regions. In our study, we compared the effects of two different adaptors (RG and Ach) on a common test stimulus in order to determine the level of selectivity of the neural responses to the test stimulus. In some previous studies, the approach was reversed and the effect of a single adaptor on two different test stimuli was compared, e.g. the effect of Ach adaptation on an RG and Ach test stimulus (Engel & Furmanski, 2001; Engel, 2005). Although we can treat our data with either approach, we consider the previous approach of comparing the effect of one adaptor on two different test stimuli to be less suited to revealing the selective nature of the driver responses as there is no reason to assume that responses to chromatic and Ach test stimuli are driven by the same neural populations. In fact, it is reasonable to assume that different neural populations may underlie the detection of chromatic and Ach test stimuli, depending on the visual area concerned.

Responses in area V1

It has been well established in the fMRI literature that V1 has a strong response to colour as well as Ach contrast (Engel *et al.*, 1997; Hadjikhani *et al.*, 1998; Beauchamp *et al.*, 1999; Brewer *et al.*, 2005; Liu & Wandell, 2005; Mullen *et al.*, 2007; Wade *et al.* 2008; Parkes *et al.*, 2009). Here, we show that in area V1 there is no evidence that the processing of either RG or Ach responses is selective. This implies that, within voxels, neurons responsive to colour are also responsive to Ach contrast, and vice versa. The lack of colour selectivity indicates that a high proportion of colour-responsive neurons are of the colour-luminance type, supporting an integrated model of processing for RG-colour contrast. This suggests that a cue-invariant processing of form, using orientation-selective mechanisms sensitive to colour and Ach contrast, is likely in V1 (Sumner *et al.*, 2008; McDonald *et al.*, 2010; Seymour *et al.*, 2010). An integrated model of colour-luminance processing is also compatible with physiological results in primates, discussed in the Introduction, showing that a large majority of the colour-sensitive neurons in primate V1 also responds well to Ach contrast. Our results, however, do not exclude the presence of a smaller sub-population of colour-selective neurons whose responses are swamped by the unselective responses when fMRI signals are averaged within the voxel or within the ROI. The limitations of the method mean that we only obtain a picture of the dominant characteristics of the visual area for the particular spatiotemporal stimuli used. Our stimuli of relatively low spatial and temporal frequency (0.5 cpd, 2 Hz) potentially activate both colour-only and colour-luminance neural populations (Schluppeck & Engel, 2002), but probably favour the responses of the minority, colour-only neurons that are typically spatially lowpass (Shapley & Hawken, 2011). Despite this, colour-selective responses are not evident in our experiments.

It is interesting that in V1 we found no evidence for selective responses to Ach test stimuli, with Ach responses adapted by both RG and Ach adaptors, presumably reflecting a dominant role of the colour-luminance responses in the BOLD signal to our Ach stimuli. This is surprising given the previous results reported from the macaque V1, showing that around half of all neurons respond exclusively to Ach contrast (Johnson *et al.*, 2004; Shapley & Hawken, 2011). Given that we did not find Ach selectivity, we speculate that Ach neurons without cone opponency may be relatively more active at spatial or temporal frequencies higher than those that we have used. If this were true, we would expect Ach selectivity to be revealed for stimuli with higher spatial or temporal frequencies. We note that V2 has a higher selectivity index than V1 for Ach stimuli, although it does not reach significance, suggesting that Ach-only responses may be more dominant in V2 than V1. In addition, there may be species differences between human and non-human primate responses.

In an earlier adaptation study, Engel & Furmanski (2001) compared the effects of one adaptor on two different types of test stimulus (RG and Ach) for single grating stimuli in V1. They, like us, found that the Ach adaptor has similar effects on both RG and Ach stimuli. Unlike us, however, they reported a stronger effect of the RG adaptor on RG chromatic than Ach stimuli, and interpreted this result to reflect colour selectivity. Subsequently, Engel (2005) showed that chromatic adaptation effects combine orientated and non-oriented components. As noted earlier, however, this strategy may not effectively reveal selectivity because the comparison is between two different types of driver response (RG and Ach) to one

adaptor, and each may be detected by a different underlying neural mechanism. Instead, the selectivity of driver responses will best be revealed by comparing the effects of two adaptors on one test stimulus, as we have done here.

Colour responses in the human ventral visual pathway

In the areas of the ventral cortex, areas V4 and especially VO exhibit a trend for increasing selectivity for RG-colour contrast. Voxels in VO, lying anterior to retinotopically mapped V4, have previously been shown to be colour responsive in the human cortex (Hadjikhani *et al.*, 1998; Bartels & Zeki, 2000; Brewer *et al.*, 2005; Mullen *et al.*, 2007), although this region has no clear corresponding area in non-human primates (Lafer-Sousa & Conway, 2013). Both here and in previous work (Mullen *et al.*, 2007) we defined an area called VO functionally by its significantly stronger response to colour (L/M cone opponent and S cone) than to Ach contrast for stimuli equated in cone contrast. We note that equating stimuli in terms of their input contrasts is crucial for a valid, quantitative comparison of chromatic and Ach responses. On this basis, VO could be functionally distinguished from V4, which overall (as an ROI) had a less differential response to colour and Ach contrast (Mullen *et al.*, 2007). This approach is not the same as contrasting responses to a coloured Mondrian with its luminance-only version, for which the average luminance contrast is constant between blocks but chromatic contrast is modulated so revealing voxels with any response to colour modulation. An area termed VO has also been identified using a different approach, using retinotopic (polar angle/eccentricity) mapping, that can be sub-divided into two regions that share a foveal representation (Brewer *et al.*, 2005). The reported Talairach coordinates for VO-1, rather than VO-2, seem to correspond better to the functionally identified VO cluster in Mullen *et al.* (2007) and to that identified here (Table S1), although the best correspondence of our cluster seems to be with that identified by Hadjikhani *et al.* (1998) on the basis of colour preference. Interestingly, Brewer *et al.* (2005) found that VO-1 responds better than VO-2 to colour in the central visual field, and shows no preferences for objects over faces, unlike VO-2.

Our results show a trend towards increasing colour selectivity in the ventral pathway in addition to the increasing colour responsiveness established previously. In particular, the increased colour selectivity of V4 and VO suggests the presence of a modular neural population responding exclusively to colour, and suggests that VO in addition to V4 plays a significant role in colour processing. For Ach contrast, no evidence for selectivity was found in either VO or V4, suggesting that the response to Ach contrast is dominated by colour-luminance neurons with relatively few purely Ach neural responses, at least for our stimuli. We know very little about the responses of individual neurons in related macaque cortical areas; however, in V4, colour-only shape-sensitive neurons that respond best at isoluminance have been reported (Bushnell *et al.*, 2011). Interestingly, an area located in a very broadly similar position to our VO has been shown to be responsive to object surface colour in an adaptation study of surface properties comparing colour, form and texture (Cavina-Pratesi *et al.*, 2010). Finally, an area in a broadly similar position may be active in human synesthetic colour experiences (Nunn *et al.*, 2002), although this result is controversial (van Leeuwen *et al.*, 2010; Hupe *et al.*, 2012; Hupe & Dojat, 2015).

Achromatic responses in the dorsal visual pathway

For Ach test stimuli, a trend towards selective Ach responses emerges in dorsal areas V3a and hMT+, with this effect also visible in V3d. This indicates the presence of a high proportion of Ach neurons with absent or weak colour responses. V3a and hMT+ are areas that have previously been shown to be more responsive to Ach than colour contrast (Liu & Wandell, 2005; Mullen *et al.*, 2007) and here we show that they also have a higher level of Ach selectivity. This is compatible with the established view of these areas as forming a specialized pathway for motion and the visual control of action with relatively poor responses to chromatic contrast. Even hMT+ still has a reliable response to the RG-colour test (Figs 5 and 6), and this response is unselective, adapting as much to the RG as the Ach adaptor. Previously it has been suggested, based on psychophysical results (Mullen *et al.*, 2003), that hMT+ behaves as if the chromatic stimulus is of a low Ach contrast, an effect that is compatible with the unselective nature of the colour response found here.

Supporting Information

Additional supporting information can be found in the online version of this article:
Fig. S1. Normalized signal loss.
Fig. S2. Individual subject adaptation effects (signal loss).
Fig. S3. Control analyses for test periods.
Fig. S4. Adaptor strength.
Table S1. Individual subject center of masses for V4, VO and MT.
Table S2. V1 (% BOLD signals).
Table S3. V2 (% BOLD).
Table S4. V3d (% BOLD).
Table S5. V3a (% BOLD).
Table S6. hMT+ (% BOLD).
Table S7. V3v (% BOLD).
Table S8. V4 (% BOLD).
Table S9. VO (% BOLD).

Acknowledgements

We are grateful to Ms Irem Onay for her assistance in data collection and Dr Ben Thompson for his contribution to the data analysis at an early stage of the work. We would like to thank all of our subjects for giving up their time. This work was supported by Canadian Institutes of Health Research (grant numbers MOP-10819 to K.T.M. and MOP-53346 to R.F.H.).

Abbreviations

Ach, achromatic; BOLD, blood oxygen level dependent; EPI, echo planar image; fMRI, functional magnetic resonance imaging; GLM, general linear model; hMT+, human medial temporal areas; MP-RAGE, magnetization prepared rapid acquisition 3d gradient recalled echo; RG, red–green; ROI, region of interest; TE, time of echo; TI, time of inversion; TR, time of repeat.

References

Bartels, A. & Zeki, S. (2000) The architecture of the colour centre in the human visual brain: new results and a review. *Eur. J. Neurosci.*, **12**, 172–193.
Beauchamp, M.S., Haxby, J.V., Jennings, J.E. & DeYoe, E.A. (1999) An fMRI version of the Farnsworth-Munsell 100-Hue test reveals multiple color-selective areas in human ventral occipitotemporal cortex. *Cereb Cortex.*, **9**, 257–263.
Boynton, G.M. & Finney, E.M. (2003) Orientation-specific adaptation in human visual cortex. *J. Neurosci.*, **23**, 8781–8787.
Bradley, A., Zang, L. & Thibos, L.N. (1992) Failures of isoluminance caused by ocular chromatic aberration. *Appl. Optics*, **31**, 3657–3667.
Brainard, D.H. (1997) The psychophysics toolbox. *Spat. Vis.*, **10**, 433–436.
Brewer, A.A., Liu, J., Wade, A.R. & Wandell, B.A. (2005) Visual field maps and stimulus selectivity in human ventral occipital cortex. *Nat. Neurosci.*, **8**, 1102–1109.

Bushnell, B.N. & Pasupathy, A. (2012) Shape encoding consistency across colours in primate V4. *J. Neurophysiol.*, **108**, 1299–1308.
Bushnell, B.N., Harding, P.J., Kosai, Y., Bair, W. & Pasupathy, A. (2011) Equiluminance cells in visual cortical area v4. *J. Neurosci.*, **31**, 12398–12412.
Cavina-Pratesi, C., Kentridge, R.W., Heywood, C.A. & Milner, A.D. (2010) Separate channels for processing form, texture, and colour: evidence from FMRI adaptation and visual object agnosia. *Cereb. Cortex*, **20**, 2319–2332.
Cottaris, N.P. (2003) Artifacts in spatiochromatic stimuli due to variations in preretinal absorption and axial chromatic aberration: implications for colour physiology. *J. Opt. Soc. Am. A*, **20**, 1694–1713.
Dumoulin, S.O., Bittar, R.G., Kabani, N.J., Baker, C.L. Jr, Le Goualher, G., Bruce Pike, G. & Evans, A.C. (2000) A new anatomical landmark for reliable identification of human area V5/MT: a quantitative analysis of sulcal patterning. *Cereb. Cortex*, **10**, 454–463.
Economides, J.R., Sincich, L.C., Adams, D.L. & Horton, J.C. (2011) Orientation tuning of cytochrome oxidase patches in macaque primary visual cortex. *Nat. Neurosci.*, **14**, 1574–1580.
Engel, S.A. (2005) Adaptation of oriented and unoriented colour-selective neurons in human visual areas. *Neuron*, **45**, 613–623.
Engel, S.A. & Furmanski, C.S. (2001) Selective adaptation to colour contrast in human primary visual cortex. *J. Neurosci.*, **21**, 3949–3954.
Engel, S.A., Rumelhart, D.E., Wandell, B.A., Lee, A.T., Glover, G.H., Chichilnisky, E.J. & Shadlen, M.N. (1994) fMRI of human visual cortex. *Nature*, **369**, 525.
Engel, S., Zhang, X. & Wandell, B. (1997) Colour tuning in human visual cortex measured with functional magnetic resonance imaging. *Nature*, **388**, 68–71.
Fang, F., Murray, S.O., Kersten, D. & He, S. (2005) Orientation-tuned FMRI adaptation in human visual cortex. *J. Neurophysiol.*, **94**, 4188–4195.
Friedman, H.S., Zhou, H. & von der Heydt, R. (2003) The coding of uniform colour figures in monkey visual cortex. *J. Physiol.*, **548**, 593–613.
Gheiratmand, M. & Mullen, K.T. (2014) Orientation tuning in human colour vision at detection threshold. *Sci. Rep.*, **4**, 4285.
Grill-Spector, K. & Malach, R. (2001) fMR-adaptation: a tool for studying the functional properties of human cortical neurons. *Acta Psychol.*, **107**, 293–321.
Hadjikhani, N., Liu, A.K., Dale, A.M., Cavanagh, P. & Tootell, R.B. (1998) Retinotopy and colour sensitivity in human visual cortical area V8. *Nat. Neurosci.*, **1**, 235–241.
Huettel, S.A., Obembe, O.O., Song, A.W. & Woldorff, M.G. (2004) The BOLD fMRI refractory effect is specific to stimulus attributes: evidence from a visual motion paradigm. *NeuroImage*, **23**, 402–408.
Hupe, J.M. & Dojat, M. (2015) A critical review of the neuroimaging literature on synesthesia. *Front. Hum. Neurosci.*, **9**, 103.
Hupe, J.M., Bordier, C. & Dojat, M. (2012) The neural bases of grapheme-colour synesthesia are not localized in real colour-sensitive areas. *Cereb. Cortex*, **22**, 1622–1633.
Johnson, E.N., Hawken, M.J. & Shapley, R. (2004) Cone inputs in macaque primary visual cortex. *J. Neurophysiol.*, **91**, 2501–2514.
Johnson, E.N., Hawken, M.J. & Shapley, R. (2008) The orientation selectivity of colour-responsive neurons in macaque V1. *J. Neurosci.*, **28**, 8096–8106.
Kourtzi, Z. & Kanwisher, N. (2000) Cortical regions involved in perceiving object shape. *J. Neurosci.*, **20**, 3310–3318.
Kourtzi, Z., Erb, M., Grodd, W. & Bulthoff, H.H. (2003) Representation of the perceived 3-D object shape in the human lateral occipital complex. *Cereb. Cortex*, **13**, 911–920.
Krekelberg, B., Boynton, G.M. & van Wezel, R.J. (2006) Adaptation: from single cells to BOLD signals. *Trends Neurosci.*, **29**, 250–256.
Lafer-Sousa, R. & Conway, B.R. (2013) Parallel, multi-stage processing of colours, faces and shapes in macaque inferior temporal cortex. *Nat. Neurosci.*, **16**, 1870–1878.
van Leeuwen, T.M., Petersson, K.M. & Hagoort, P. (2010) Synaesthetic colour in the brain: beyond colour areas. A functional magnetic resonance imaging study of synaesthetes and matched controls. *PLoS One*, **5**, e12074.
Lennie, P., Krauskopf, J. & Sclar, G. (1990) Chromatic mechanisms in striate cortex of macaque. *J. Neurosci.*, **10**, 649–669.
Leventhal, A.G., Thompson, K.G., Liu, D., Zhou, Y. & Ault, S.J. (1995) Concomitant sensitivity to orientation, direction, and colour of cells in layers 2, 3, and 4 of monkey striate cortex. *J. Neurosci.*, **15**, 1808–1818.
Levitt, J.B., Kiper, D.C. & Movshon, J.A. (1994) Receptive fields and functional architecture of macaque V2. *J. Neurophysiol.*, **71**, 2517–2542.
Li, X., Chen, Y., Lashgari, R., Bereshpolova, Y., Swadlow, H.A., Lee, B.B. & Alonso, J.M. (2015) Mixing of chromatic and luminance retinal signals in primate area V1. *Cereb. Cortex*, **25**, 1920–1937.
Liu, J. & Wandell, B.A. (2005) Specializations for chromatic and temporal signals in human visual cortex. *J. Neurosci.*, **25**, 3459–3468.
Livingstone, M.S. & Hubel, D.H. (1984) Anatomy and physiology of a colour system in the primate visual cortex. *J. Neurosci.*, **4**, 309–356.
Livingstone, M.S. & Hubel, D.H. (1988) Segregation of form, colour, movement, and depth: anatomy, physiology, and perception. *Science*, **240**, 740–749.
McDonald, J.S., Mannion, D.J., Goddard, E. & Clifford, C.W. (2010) Orientation-selective chromatic mechanisms in human visual cortex. *J. Vision*, **10**, 34.
McKeefry, D.J. & Zeki, S. (1997) The position and topography of the human colour centre as revealed by functional magnetic resonance imaging. *Brain*, **120**(Pt 12), 2229–2242.
Michna, M.L. & Mullen, K.T. (2008) The contribution of colour to global motion processing. *J. Vision*, **8**, 10.1–12.
Mullen, K.T. (1985) The contrast sensitivity of human colour vision to red-green and blue-yellow chromatic gratings. *J. Physiol.*, **359**, 381–400.
Mullen, K.T., Yoshizawa, T. & Baker, C.L. Jr (2003) Luminance mechanisms mediate the motion of red-green isoluminant gratings: the role of "temporal chromatic aberration". *Vision. Res.*, **43**, 1235–1247.
Mullen, K.T., Dumoulin, S.O., McMahon, K.L., de Zubicaray, G.I. & Hess, R.F. (2007) Selectivity of human retinotopic visual cortex to S-cone-opponent, L/M-cone-opponent and achromatic stimulation. *Eur. J. Neurosci.*, **25**, 491–502.
Mullen, K.T., Dumoulin, S.O. & Hess, R.F. (2008) Colour responses of the human lateral geniculate nucleus: selective amplification of S-cone signals between the lateral geniculate nucleno and primary visual cortex measured with high-field fMRI. *Eur. J. Neurosci.*, **28**, 1911–1923.
Mullen, K.T., Thompson, B. & Hess, R.F. (2010) Responses of the human visual cortex and LGN to achromatic and chromatic temporal modulations: an fMRI study. *J. Vision*, **10**, 13, 1–19.
Nunn, J.A., Gregory, L.J., Brammer, M., Williams, S.C., Parslow, D.M., Morgan, M.J., Morris, R.G., Bullmore, E.T., Baron-Cohen, S. & Gray, J.A. (2002) Functional magnetic resonance imaging of synesthesia: activation of V4/V8 by spoken words. *Nat. Neurosci.*, **5**, 371–375.
Parkes, L.M., Marsman, J.B., Oxley, D.C., Goulermas, J.Y. & Wuerger, S.M. (2009) Multivoxel fMRI analysis of color tuning in human primary visual cortex. *J. Vision*, **9**, 1, 1–13.
Pelli, D.G. (1997) The Videotoolbox software for visual psychophysics: transforming numbers into movies. *Spat. Vis.*, **10**, 437–442.
Schluppeck, D. & Engel, S.A. (2002) Colour opponent neurons in V1: a review and model reconciling results from imaging and single-unit recording. *J. Vision*, **2**, 480–492.
Sereno, M.I., Dale, A.M., Reppas, J.B., Kwong, K.K., Belliveau, J.W., Brady, T.J., Rosen, B.R. & Tootell, R.B. (1995) Borders of multiple visual areas in humans revealed by functional magnetic resonance imaging. *Science*, **268**, 889–893.
Seymour, K., Clifford, C.W., Logothetis, N.K. & Bartels, A. (2010) Coding and binding of colour and form in visual cortex. *Cereb. Cortex*, **20**, 1946–1954.
Shapley, R. & Hawken, M.J. (2011) Colour in the cortex: single- and double-opponent cells. *Vision. Res.*, **51**, 701–717.
Sincich, L.C. & Horton, J.C. (2005) The circuitry of V1 and V2: integration of colour, form, and motion. *Annu. Rev. Neurosci.*, **28**, 303–326.
Sumner, P., Anderson, E.J., Sylvester, R., Haynes, J.D. & Rees, G. (2008) Combined orientation and colour information in human V1 for both L-M and S-cone chromatic axes. *NeuroImage*, **39**, 814–824.
Talairach, J. & Tournoux, P. (1988) *Co-Planar Stereotaxic Atlas of the Human Brain*. Thieme, New York.
Tanigawa, H., Lu, H.D. & Roe, A.W. (2010) Functional organization for colour and orientation in macaque V4. *Nat. Neurosci.*, **13**, 1542–1548.
Thorell, L.G., De Valois, R.L. & Albrecht, D.G. (1984) Spatial mapping of monkey V1 cells with pure colour and luminance stimuli. *Vision. Res.*, **24**, 751–769.
Vaughan, J.T., Adriany, G., Garwood, M., Yacoub, E., Duong, T., DelaBarre, L., Andersen, P. & Ugurbil, K. (2002) Detunable transverse electromagnetic (TEM) volume coil for high-field NMR. *Magn. Reson. Med.*, **47**, 990–1000.
Wade, A., Augath, M., Logothetis, N. & Wandell, B. (2008) fMRI measurements of color in macaque and human. *J. Vision*, **8**, 6, 1–19.